Mass Transfer Between a Flowing Fluid and a Solid Wavy Surface

CHARLES B. THORSNESS
and
THOMAS J. HANRATTY
Department of Chemical Engineering
University of Illinois
Urbana, Illinois 61801

This paper considers the transfer of mass or heat between a fluid and a small amplitude solid wavy surface. A periodic variation of the transfer rate can occur because of wave induced variations of the normal convective flow and of the properties of the turbulence. Solutions of the mass balance equations are presented for the laminar flow at a large Schmidt number or Prandtl number and for turbulent flow at large and small wave numbers. For turbulent flows at intermediate wave numbers, the prediction is limited by inadequacies of present theories that model the wave induced variation in the turbulent diffusion of heat or mass. In order to provide guidance for this modeling, new measurements on the variation of the mass transfer rate along a solid wavy surface are presented for a Schmidt number of 729. An analogy between momentum and mass transfer is explored as a means for evaluating the turbulent diffusion terms.

The amplitude of the function describing the mass transfer variation is found to decrease with decreasing wave number and the phase to increase with decreasing wave number. The phase angle and the amplitude of the variation in the mass transfer rate relative to the average mass transfer rate are insensitive to changes in Schmidt number or Prandtl number. For turbulent flows, the phase change can be large enough that the maximum in the mass transfer rate can exist somewhere in the trough of the wave. This result is of considerable significance in interpreting wavelike dissolution patterns.

SCOPE

The flow of fluid over a soluble solid wavy surface is accompanied by a spatial variation of the rate of solution. For sinusoidal waves of small enough amplitude, a linear response can be expected in that the spatial average mass transfer rate is the same as for a flat surface, and the variation from this average has a single harmonic with the same wavelength as the surface. For a laminar flow, this spatial variation is caused principally by a periodic convective flow normal to the surface induced by the wave. For a turbulent flow, the induced variation of the Reynolds transport is an additional mechanism which can dominate that due to convective motion associated with the average flow.

Considerable attention has been given to induced perturbations of the velocity field caused by small amplitude solid waves on a wall. In particular, the analysis by Benjamin (1959) should be cited. No previous work has been done on the mass transfer problem. In this paper, we use the analysis of Benjamin, as well as more recent studies, to predict the wave induced variation of the concentration field and of the mass transfer rate along the surface.

The chief theoretical problem in carrying out the analysis for turbulent flows is the evaluation of the Reynolds transport term. In order to determine the accuracy of the mass transfer analogy used for this purpose, new experimental results were obtained for turbulent mass transfer to small amplitude waves for a Schmidt number equal to 729. In addition, the measurements by Ashton and Kennedy (1972) for the melting of ice provided results for a Prandtl number equal to 13.7. The studies of mass transfer rates to wavy surfaces by Verma and Cermak (1974) were done for waves of too large an amplitude for our analysis to be applicable.

The results of this paper could be of considerable interest in interpretating the influence of wavy surfaces on average mass transfer rates. However, for this purpose the analysis would have to be extended over a wider range of wave amplitudes. The principal motivation has been to predict the stability of dissolving surfaces. Of extreme importance to the stability problem is the phase of the spatial variation of the mass transfer rate. In fact, a necessary condition for instability of dissolving surfaces is that the maximum in the mass transfer rate occurs somewhere in the trough of the wave.

Charles B. Thorsness is with Lawrence Livermore Laboratory, Livermore, California.

0065-8812-79-2711-0686-$01.35.

CONCLUSIONS AND SIGNIFICANCE

For both laminar and turbulent boundary layers, small amplitude wavy surfaces can cause a spatial variation of the mass transfer rate of large amplitude compared to the spatially averaged mass transfer rate. The maximum in the mass transfer rate can be shifted a considerable distance upstream of the crest of the wave. The amplitude of the function describing the mass transfer variation decreases with decreasing wave number, and the phase (relative to the wave crest) increases with decreasing wave number. Both the amplitude and the phase are relatively insensitive to changes in the Schmidt number or Prandtl number.

The phase angle of the mass transfer variation is larger for turbulent flows than for laminar flows. For dimensionless wave number α less than approximately 2×10^{-3}, the phase angle can be greater than 90 deg for turbulent flows. A maximum in the mass transfer rate can therefore exist in the wave trough, so dissolution instabilities are possible.

For turbulent boundary layers, the turbulent transport terms are evaluated by assuming that the local eddy diffusion coefficient is proportional to the local eddy viscosity. It is found that this modeling of the wave induced Reynolds transport terms is important only at intermediate wave numbers. At large wave numbers the concentration boundary layer is thin enough that turbulent transport is negligible, and at small wave numbers the local mass transfer rate is the same as for a flat plate with a wall shear stress equal to the local stress on the wave surface. The agreement of predictions of the phase and the amplitude of the mass transfer variation for a turbulent field with experimental results is satisfactory but not exact. We have tentatively concluded that further improvements in the modeling will require abandoning the use of an analogy between wave induced momentum and scalar transport.

The profile of a sinusoidal surface is represented in Cartesian coordinates as

$$Y = a \cos(\alpha X) \tag{1}$$

For a linear system, the spatial variation of the mass flux to the surface is given as

$$N(X) = \overline{N} + a|\hat{n}| \cos(\alpha X + \theta) \tag{2}$$

The goals of this work are to evaluate $a|\hat{n}|$ and θ by solving the linearized mass balance equation and to present new experimental results for turbulent mass transfer which can be used to verify these solutions.

For laminar fields, the wave induced flow can be obtained from the solution of the linearized momentum equations presented by Benjamin (1959). For turbulent fields, the solution of the momentum equations and the mass balance equation depends on how well the Reynolds transport terms can be approximated. In previous papers (Thorsness and Hanratty, 1977; Thorsness, Morrisroe, and Hanratty, 1978), and in a thesis by one of the authors (Thorsness, 1975) we have examined the accuracy with which a number of models of the eddy viscosity can be used to calculate wave induced flow by comparing measured and predicted shear stress variations along a wavy wall. We found that a modified version of the Van Driest relation, the eddy viscosity relation of Loyd, Moffat, and Kays (1970), did a satisfactory job and, therefore, have used this model to calculate the velocity field for turbulent flows. We evaluate the influence of turbulence on the transport of heat and mass by using an analogy whereby we assume that the turbulent diffusivity of heat or mass is proportional to the Loyd, Moffat, and Kays eddy viscosity.

The accuracy of the calculations for turbulent flow is examined by comparing them with measurements of the melting of ice by Ashton and Kennedy (1972) and with measurements of mass transfer by electrochemical techniques recently obtained in a Ph.D. thesis by Thorsness (1975). Ashton and Kennedy carefully measured the changes in the profiles of small amplitude waves on ice surfaces that are melting into a flowing stream of water and calculated local values of the heat transfer rate. Thorsness used a portion of a wavy wall over which a liquid was flowing as one of the electrodes in an electrolysis cell. The cell was operated under conditions so that the current flow was controlled by the rate of mass transfer to the wavy electrode. The variation of the mass transfer rate along the surface was determined by measuring the current flowing to a series of wires embedded flush with the electrode surface but insulated from it.

LINEARIZED MASS BALANCE

The problem considered for analysis is that of a fluid of infinite extent flowing over a solid wavy surface. The velocity of the fluid at large distances from the surface has a magnitude U_∞ and contains the scalar quantity being exchanged with the wave surface at a concentration S_∞. The concentration of this scalar is kept at some fixed value along the wave surface, different from that at a large distance.

The mass balance is formulated in a boundary-layer coordinate system in which the x direction is parallel to the wave surface and the y direction perpendicular to it. Velocities are made dimensionless with respect to a friction velocity $u^* = (\overline{\tau}_W/\rho)^{1/2}$ defined in terms of a wall shear stress averaged over a wavelength, lengths, with respect to the ratio of the kinematic viscosity to the friction velocity ν/u^*, and pressures and stresses with respect to ρu^{*2}. The concentration of the scalar quantity being transferred (S) is defined relative to its value at the wave surface, so that $S_W = 0$. The concentration is made dimensionless using the ratio of the average flux along the wave surface to the friction velocity $\overline{N}/u^*$ and scalar fluxes with respect to $\overline{N}$.

We use a boundary-layer assumption, whereby the influence of turbulent and molecular diffusion terms in the x direction is ignored. The scalar balance equation is then

$$\frac{1}{h_x}U\frac{\partial S}{\partial x}+\frac{1}{h_y}V\frac{\partial S}{\partial y}$$
$$=\frac{1}{h_xh_y}\left[\frac{1}{Z}\frac{\partial}{\partial y}\left(\frac{h_x}{h_y}\frac{\partial S}{\partial y}\right)+\frac{\partial}{\partial y}(h_xM)\right] \quad (3)$$

where h_x and h_y are the metrics for the boundary layer coordinate system, which to order a are given as

$$h_y=1 \quad (4)$$
$$h_x=1+a\alpha^2ye^{i\alpha x} \quad (5)$$

A more complete discussion of the derivation of (3) can be found in the thesis by Thorsness (1975).

For a linear response, the time averaged velocity, concentration, and Reynolds transport at a fixed value of y are given as the sum of the average over a wavelength and of a wave induced component having the same wave number as the profile of the solid surface:

$$U=\overline{U}(y)+a\hat{u}(y)e^{i\alpha x} \quad (6)$$
$$V=\overline{V}(y)+a\hat{v}(y)e^{i\alpha x} \quad (7)$$
$$S=\overline{S}(y)+a\hat{s}(y)e^{i\alpha x} \quad (8)$$
$$M=\overline{M}(y)+a\hat{m}(y)e^{i\alpha x} \quad (9)$$

where a and α are real, and $\hat{u}$, $\hat{v}$, $\hat{s}$, $\hat{m}$ can be complex. Since for a linear response the amplitudes of the wave induced changes vary linearly with wave amplitude, we have chosen to show this dependency explicitly. Thus, $a\hat{u}(y)$ is the amplitude of the wave induced variation of U, and $\hat{u}(y)$ is independent of a. The above equations imply that the changes of U, V, S, and M are small over one wavelength and, consequently, that the thicknesses of the velocity and concentration boundary layers do not change appreciably over one wavelength.

Equations (4), (5), (6), (7), (8), and (9) are substituted into (3), and terms of order a^2 are neglected. The following equation is derived for $\hat{s}(y)$, where primes denote differentiation with respect to y:

$$e^{i\alpha x}\left[i\alpha\overline{U}a\hat{s}+a\hat{v}\overline{S}'+a\hat{u}\frac{\partial\overline{S}}{\partial x}+\overline{V}a\hat{s}'\right]$$
$$+\overline{U}\frac{\partial\overline{S}}{\partial x}+\overline{V}\overline{S}'=\frac{1}{Z}\overline{S}''+\overline{M}'+\left[\frac{a}{Z}(\hat{s}'')+a\hat{m}'\right.$$
$$\left.+a\alpha^2\left(y\overline{U}\frac{\partial\overline{S}}{\partial x}+\overline{M}+\frac{1}{Z}\overline{S}'\right)\right]e^{i\alpha x} \quad (10)$$

The last three terms on the right side of (10) arise because of the curvature of the coordinate system. They can be important only for very large α, where induced variations of concentration are confined to a region over which the $\overline{S}$ is varying linearly with y. Consequently, from (15) we see that we can approximate these three terms as equal to α^2.

Using this approximation, we find that we can neglect these terms since they can be important only for $\alpha > 1$ which is outside the range of interest in this work. In addition, we are interested in fully developed flows in a channel or in boundary layers that are sufficiently developed that $\hat{u}\frac{\partial\overline{S}}{\partial x}$ and $\overline{V}\hat{s}'$ in (10) can be neglected.

The spatial average of (10) is given as

$$\overline{U}\frac{\partial\overline{S}}{\partial x}+\overline{V}\overline{S}'=\frac{1}{Z}\overline{S}''+\overline{M}' \quad (11)$$

Subtraction of (11) from (10) simplifies the mass balance to

$$i\alpha\overline{U}\hat{s}+\hat{v}\overline{S}'=\frac{1}{Z}\hat{s}''+\hat{m}' \quad (12)$$

The equation for $\hat{s}(y)$ is to be solved using the boundary conditions

$$\hat{s}(0)=\hat{s}(\infty)=0 \quad (13)$$

From this solution, the mass or heat flux at the surface is calculated from

$$\left.\frac{1}{h_y}\frac{\partial S}{\partial y}\right|_{y=0}=\overline{S}'(0)+a\hat{s}'(0)e^{i\alpha x} \quad (14)$$

From the manner in which the variables were made dimensionless

$$\overline{S}'(0)=Z \quad (15)$$
$$\frac{a\hat{s}'(0)}{Z}e^{i\alpha x}=\frac{a\hat{n}}{\overline{N}}e^{i\alpha x} \quad (16)$$

$\overline{N}=1$, and complex amplitude function $\hat{n}$ has been normalized with $\overline{N}u^*/\nu$.

LAMINAR FLOWS WITH LARGE SCHMIDT OR PRANDTL NUMBER

We now consider a laminar flow solution of (12), for which $\hat{m}$ and $\overline{M}$ are zero, using large values of the Schmidt number or Prandtl number Z. Under these circumstances, the scalar boundary layer is much thinner than the velocity boundary layer, so that the velocity field may be taken as $\overline{U}=y$, $\hat{v}(y)=\hat{v}''(0)\,y^2/2$. The variation of the mean scalar is assumed to have a form which satisfies (15) and the conditions that $\overline{S}(0)=0$, $\overline{S}'=\overline{S}''=0$ for $y/\delta_c>1$:

$$\overline{S}=\left[2\left(\frac{y}{\delta_c}\right)-2\left(\frac{y}{\delta_c}\right)^3+\left(\frac{y}{\delta_c}\right)^4\right]\frac{\delta_cZ}{2} \quad (17)$$

The simplified form of (12) to be solved is

$$i\alpha y\hat{s}-i\alpha\frac{1}{2}\frac{\hat{\tau}_W}{\overline{\tau}_W}y^2Z\left[1-3\left(\frac{y}{\delta_c}\right)^2\right.$$
$$\left.+2\left(\frac{y}{\delta_c}\right)^3\right]=\frac{1}{Z}\hat{s}'' \quad (18)$$

where $|a\hat{\tau}_W|$ is the wave induced amplitude of the wall shear stress, and the relation $\hat{v}''(0)=-i\alpha\hat{\tau}_W/\overline{\tau}_W$ has been used. It is to be noted that from the manner in which terms have been made dimensionless, $\overline{\tau}_W=1$ and the complex amplitude function $\hat{\tau}_W$ has been normalized with $\overline{\tau}_Wu^*/\nu$.

By using the method of variation of parameters, we find that

$$\frac{\hat{n}}{\overline{N}}=\frac{\hat{s}'(0)}{Z}=+\frac{i\frac{\hat{\tau}_W}{\overline{\tau}_W}}{2Ai(0)}\int_0^{\delta_c^*}Ai(y^*i^{1/3})y^{*2}$$

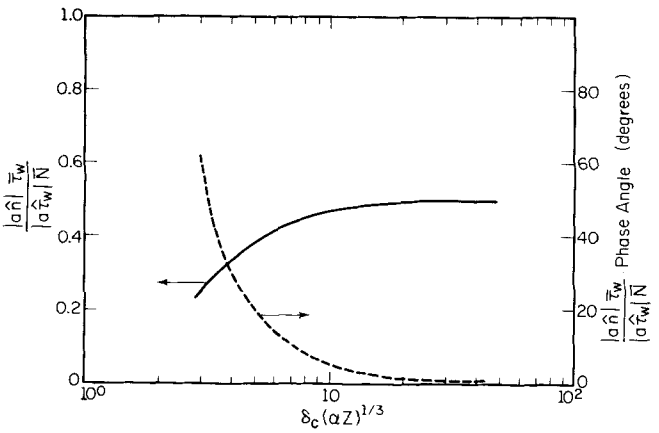

Fig. 1. Calculated amplitudes and phase angles of the mass transfer variation for laminar flow.

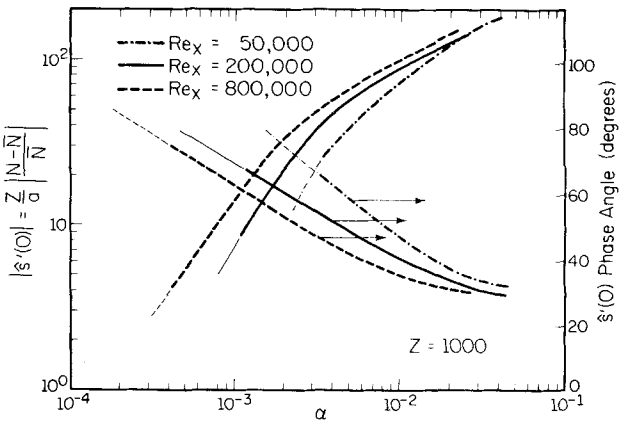

Fig. 2. Calculated values of amplitude and phase of s' (0) for laminar flow.

$$\left[1-3\left(\frac{y}{\delta_c}\right)^2+2\left(\frac{y}{\delta_c}\right)^3\right]dy^* \quad (19)$$

where $y^* = (\alpha Z)^{1/3}y$ and $\delta_c^* = (\alpha Z)^{1/3}\delta_c$. It is apparent from the above result that the magnitude and phase of the wave induced mass transfer rate relative to that of the wave induced wall shear stress variation is a function of $(aZ)^{1/3}\delta_c$. Thorsness has evaluated (19) numerically to yield the results shown in Figure 1. It is noted that at large α the normalized wave induced mass transfer variation has the same magnitude and phase as the normalized variation in wall shear stress. With decreasing α there is an increase in the relative phase angle, so that the maximum mass transfer rate precedes the maximum shear stress.

However, the above results might not have much meaning for very small values of α, where the wavelength is of the same order as the length of the plate required to develop the boundary layer. The condition of $x = \lambda$ for a case for which the thicknesses of the hydrodynamic and scalar boundary layers are given by

$$\delta = 2.75Re_x^{1/4} \quad (20)$$

$$\frac{\delta}{\delta_c} = Z^{1/3} \quad (21)$$

is

$$\alpha_{MIN} = \frac{3.64\pi}{Re_x^{3/4}} \quad (22)$$

It is necessary to calculate $\hat{\tau}_W/\bar{\tau}_W$ in order to evaluate the magnitude of $\hat{n}/\bar{N}$ and its phase relative to the wave profile. For this purpose, the linearized momentum equations presented by Benjamin (1959) for laminar boundary layers are used. Thorsness (1975) has solved these equations using the average velocity profile suggested by Benjamin:

$$\bar{U} = \frac{2\delta}{\pi}\sin\left(\frac{\pi}{2}\frac{y}{\delta}\right) \quad 0<y<\delta$$

$$\bar{U} = \frac{2\delta}{\pi} \quad \delta<y \quad (23)$$

The calculated value of $\hat{\tau}_W/\bar{\tau}_W$ depends on α and δ. If the results of this calculation are used in (19) and the concentration and velocity boundary layers are assumed to have the properties indicated by (20), (21), and (22), the amplitude and the phase of the wave induced mass transfer variations shown in Figure 2 are calculated. It is noted in Figure 2 that at large values of α the wave induced variation of mass flux is quite large, being equal to about 0.1 to 0.2 of the mean flux for waves with amplitude $a = 1$. The phase angle, which is largely governed by the phase angles of the wall shear stress variation, has values between 30 and 70 deg.

TURBULENT FLOWS

Solutions of (12) will be presented for turbulent flows that are sufficiently developed that the variation of mean scalar field is given as a solution of

$$\frac{1}{Z}\bar{S}' + \bar{M} = 1 \quad (24)$$

If an eddy diffusivity is defined as

$$\bar{M} = \frac{\bar{\epsilon}}{\nu}\bar{S}' \quad (25)$$

the mean scalar field is obtained by integrating (24):

$$\bar{S} = \int_0^y \frac{dy}{\frac{1}{Z}+\frac{\bar{\epsilon}}{\nu}} \quad (26)$$

The use of the Van Driest eddy viscosity function with a turbulent Prandtl number of unity was found by Thorsness (1975) to give profiles of $\bar{S}$ which are consistent with the measurements of mass transfer rates at large Schmidt numbers by Harriot and Hamilton (1965) and by Hubbard (1968) and the measurements of heat transfer rates at a Prandtl number of 8 by Allen and Eckert (1964):

$$\frac{\bar{\epsilon}}{\nu} = \frac{\bar{\nu}_T}{\nu} = (\kappa y)^2\left[1-\exp\left(-\frac{y}{A}\right)\right]^2\bar{U}' \quad (27)$$

$\kappa = 0.41$, and $A = 25$. For a constant stress boundary layer, this model leads to the following relation for $\bar{U}$:

$$\bar{U} = \int_0^y \frac{2dy}{1+\sqrt{1+\kappa^2y^2\left[1-\exp\left(-\frac{y}{A}\right)\right]^2}} \quad (28)$$

Two methods for handling the evaluation of the wave induced variation of the transport are used. One of these is the quasilaminar assumption that $\hat{m} = 0$. The other uses an analogy between momentum transport and mass

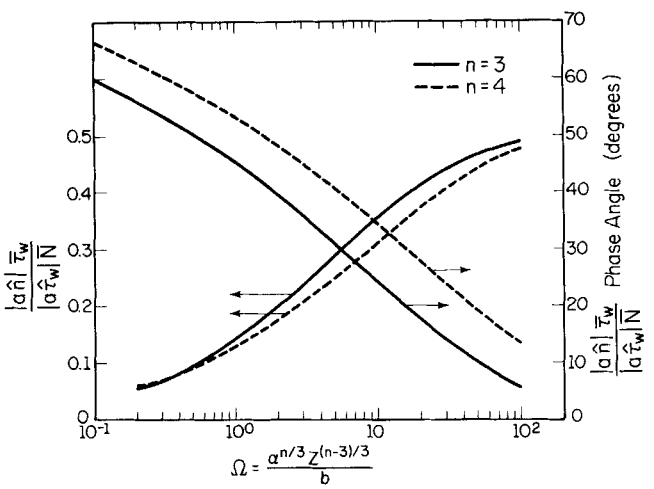

Fig. 3. Quasilaminar solution for turbulent mass transfer to wavy surfaces at large Schmidt number, Z.

transport, whereby the eddy diffusivity of heat or mass ϵ is assumed proportional to the eddy viscosity ν_T:

$$\frac{\hat{\epsilon}}{\hat{\nu}_T} = \frac{\bar{\epsilon}}{\bar{\nu}_T} = \frac{1}{Z_T} \tag{29}$$

$\hat{\epsilon}$ and $\hat{\nu}_T$ are dimensional quantities defined by

$$\frac{\epsilon}{\nu} = \frac{\bar{\epsilon}}{\nu} + \frac{a\hat{\epsilon}}{u^*} e^{i\alpha x} \tag{30}$$

$$\frac{\nu_T}{\nu} = \frac{\bar{\nu}_T}{\nu} + \frac{a\hat{\nu}_T}{u^*} e^{i\alpha x} \tag{31}$$

Since $M = \epsilon/\nu S'$, it follows from the assumption (29) that

$$\hat{m} = \frac{\bar{\nu}_T}{Z_T}\hat{s}' + \frac{\hat{\nu}_T}{u^* Z_T}\overline{S'} \tag{32}$$

According to the quasilaminar model, the variation of mass transfer along the wave surface is caused by velocities normal to the surface induced by the wave, the term $\hat{v}\,\overline{S'}$ in (12). The inclusion of turbulent transport terms allows for a variation of mass transfer due to wave induced variations in m, $\hat{m}'$ in (12), as well as in the velocity field.

The wave induced variation of the velocity field is obtained from the solution of the linearized momentum equations given by Thorsness et al. (1978) for the boundary-layer coordinate system. This solution requires the specification of the variation of eddy viscosity. Thorsness et al. (1978) have compared a number of models for ν_T/ν with respect to their ability to predict the variation of the wall shear stress along the wave surface and found that a modified version of the Van Driest relation presented by Loyd, Moffat, and Kays (1970) did a satisfactory job. According to this model

$$\frac{\nu_T}{\nu} = L^2(2e_{xy}) \tag{33}$$

and

$$L = \kappa y\left[1 - \exp\left(-\frac{y}{A}\right)\left(\frac{\tau_W}{\bar{\tau}_W}\right)^{1/2}\right] \tag{34}$$

where A, which is a measure of the thickness of the viscous wall region, is a function of the pressure gradient. For equilibrium boundary layers, where the pressure gradient is not varying, A increases in favorable pressure gradients and decreases in unfavorable pressure gradients. For small enough pressure gradients

$$A = A_0\left(1 + k_1\frac{dp}{dx}\right) \tag{35}$$

where k_1 is a negative number. For nonequilibrium flows, Loyd et al. (1970) have argued that an effective pressure gradient $(dp/dx)_{\text{eff}}$ should be used in (35):

$$\frac{d\left(\frac{dp}{dx}\right)_{\text{eff}}}{dx} = \frac{\left(\frac{dp}{dx}\right) - \left(\frac{dp}{dx}\right)_{\text{eff}}}{k_L} \tag{36}$$

According to this model, wave induced variations in turbulent transport of heat, mass, or momentum occur because of variation in S', e_{xy}, dp/dx, and $\tau_W/\bar{\tau}_W$. The turbulent transport terms are made to respond instantaneously to changes in S', e_{xy}, and τ_W but are relaxed with respect to changes in dp/dx. This is identified as model D in the paper by Thorsness, Morrisroe, and Hanratty (1978). Loyd et al. (1970) suggested that $\kappa = 0.41$, $\overline{A} = 25$, $k_1 = -30$, and $k_L = 3\,000$. Thorsness, Morrisroe, and Hanratty found that the use of these values gave approximate agreement between the measured and predicted variation of the wall shear stress along the wave surface. However, much closer agreement could be obtained if values of $k_1 = -60$, $k_L = 3\,000$ or $k_1 = -30$, $k_L = 1\,500$ were used.

SPECIAL SOLUTIONS FOR TURBULENT FLOW

Quasilaminar Solution for Very Large Schmidt or Prandtl Numbers

The solution of the turbulent mass balance Equation (12) for very large Z using the quasilaminar assumption $\hat{m} = 0$ produces results quite similar to those presented previously. The only difference is in the specification of $\overline{S}(y)$. For very large Z, average temperature and concentration profiles are usually calculated from (26) by representing the turbulent diffusivity by the following power law:

$$\frac{\bar{\epsilon}}{\nu} = by^n \tag{37}$$

For the Van Driest relation, (27), with $\kappa = 0.41$ and $A = 25$, $b = 0.000269$ and $n = 4$. However, values of $n = 3$ and $b = 0.00049$ have been suggested by Hughmark (1972) and values of $n = 3.38$ and $b = 0.000463$ by Shaw and Hanratty (1977).

The solution of (12) with $\hat{m}' = 0$ and $\overline{S}$ defined by (26) and (37) is

$$\frac{\hat{n}}{N} = \frac{i\hat{\tau}_W}{2Ai(0)\,\bar{\tau}_W}\int_0^\infty y^{*2}\left[1 + \frac{y^{*n}}{\Omega}\right]^{-1} Ai(y^* i^{1/3})\,dy^* \tag{38}$$

$$\Omega = \frac{a^{n/3} Z^{\frac{n-3}{3}}}{b} \tag{39}$$

The amplitude and phase of $\hat{n}\,\bar{\tau}_W/\bar{N}\,\hat{\tau}_W$ calculated from (38) are given in Figure 3 as a function of Ω. It is to be

noted $\hat{n}/\bar{N}$ is independent of Z for $n = 3$ and only weakly dependent on it for $n = 4$.

Solution for Large α

For large enough α, the wave induced variation in the concentration is confined to a small region close to the wall where the variation of the average scalar quantity $\bar{S}$ is given by a linear relation, and turbulence has no effect. Consequently, limiting behavior at large α is given by solving (12) with $\hat{m}' = 0$ and $\bar{S}' = Z$. The result is Equation (38) with $\Omega = \infty$ or (19) with $\delta_c^* = \infty$. The relation of $\hat{n}/\bar{N}$ and $\hat{\tau}_W/\bar{\tau}_W$ for turbulent flows at large α is, therefore, the same as what had been found previously for laminar flows at large α. That is, the relative phase of $\hat{n}/\bar{N}$ and $\hat{\tau}_W/\bar{\tau}_W$ is zero, and the ratio $\hat{n}/\bar{N}$ to $\hat{\tau}_W/\bar{\tau}_W$ equals 0.5.

Solution for $\alpha \to 0$ and for Large Z

A solution for $\alpha \to 0$ can be obtained for fluids with large Z by assuming that the local mass transfer rate is the same as for a flat surface.

The average mass transfer coefficient for fully developed conditions is given as

$$\frac{\bar{K}}{u^*} = f(Re, Z) \tag{40}$$

For large Z, Equation (40) can be simplified to

$$K = \left(\frac{\bar{\tau}_W}{\rho}\right)^{1/2} g(Z) \tag{41}$$

For $\alpha \to 0$, the rate of change of the flow field along the wave is so slow that it can be assumed that

$$K = \left(\frac{\tau_W}{\rho}\right)^{1/2} g(Z) \tag{42}$$

If $K = \bar{K} + k$ and $\tau_W = \bar{\tau}_W + \tau_W'$ are substituted into (42) and it is assumed that $\tau_W'/\bar{\tau}_W$ and $k/\bar{K}$ are small, then it can be shown that

$$\frac{k}{\bar{K}} = \frac{1}{2}\frac{\tau_W'}{\bar{\tau}_W} = \frac{1}{2}\frac{\hat{\tau}_W}{\bar{\tau}_W} ae^{i\alpha x} \tag{43}$$

From (41) and (43), it follows that

$$\frac{\hat{n}}{\bar{N}} = \frac{1}{2}\frac{\hat{\tau}_W}{\bar{\tau}_W} \tag{44}$$

The wave induced variation in the mass transfer variations are in phase with the wave induced variation in the wall shear stress, and the ratio of the amplitudes is equal to one half the ratio $\bar{N}/\bar{\tau}_W$.

DESCRIPTION OF MASS TRANSFER EXPERIMENTS

The experimental studies of mass transfer to wavy surfaces were carried out in a 5.08 cm by 61 cm rectangular channel that is 8.38 m long. The test section was 61 cm × 68.6 cm, with the removable part of the lower wall located at the outlet end of the channel where the flow is fully developed. It consists of a train of ten waves machined into a 3.175 cm × 61 cm × 68.6 cm lucite slab. The waves have an amplitude (one-half of the distance between the crest and trough) of 0.03175 cm and a length of 5.08 cm. A brass 10.16 cm × 20.3 cm insert is

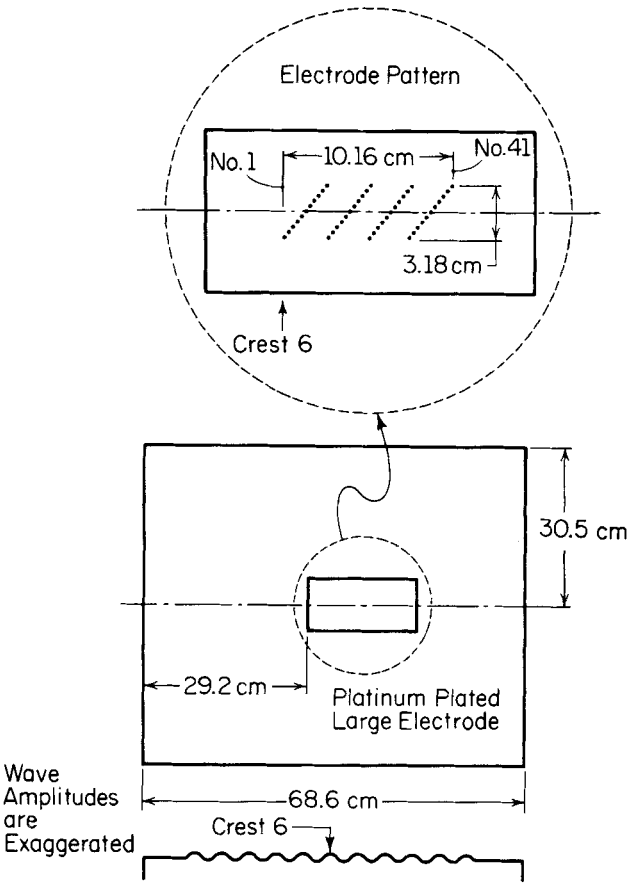

Fig. 4. Pattern of test electrodes used in the experiments.

TABLE 1. PHYSICAL AND CHEMICAL PROPERTIES OF ELECTROLYTE SYSTEM

Property	Iodine system
Viscosity, kg/ms	8.72×10^{-4}
Density, kg/m³	1 023
Kinematic viscosity, m²/s	8.52×10^{-7}
Mass diffusivity, m²/s	1.168×10^{-9}
Schmidt number	729
KI Concentration, mole/m³	103
$I_2(I_3)$ concentration, mole/m³	1.29 -1.51

located in the middle of this test section and contoured to the shape of the waves. This insert was plated with platinum and used as the cathode of an electrolytic cell. The anode was the stainless steel channel and holding tank which were part of the flow loop.

An electrolyte consisting of iodine dissolved in a 0.1 molar potassium iodide solution was circulated through the flow loop. The concentration of iodine was approximately 0.0013 molar. A voltage was applied between the anode and cathode, and the following reactions took place:

$$\text{(cathode)} \quad I_3^- + 2e^- \rightarrow 3I^-$$

$$\text{(anode)} \quad 3I^- \rightarrow I_3^- + 2e^-$$

At large enough voltages, the reaction at the cathode is rapid enough that the current flowing in the circuit is controlled by the rate of mass transfer to the cathode surface. Under these circumstances, flux to the cathode surface N is related to the electrical current I by

$$N = \frac{I}{A_e n_e S_\infty F} \tag{45}$$

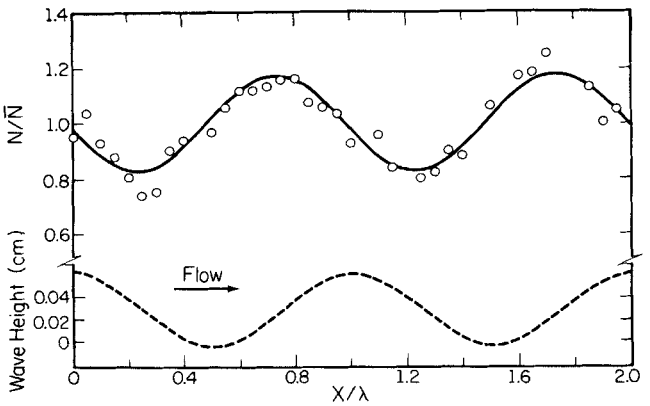

Fig. 5. Wall shear stress variation along a wavy surface for *Re* = 25 200.

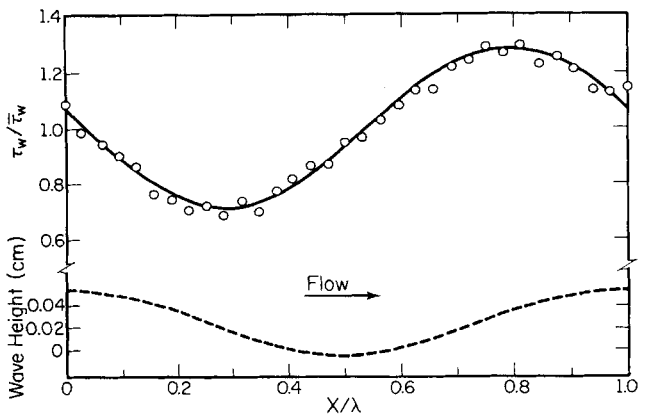

Fig. 7. Mass transfer variation along a wavy surface for *Re* = 20 900.

Local values of the mass flux along the wave surface were determined by measuring the current to 0.064 cm diameter platinum wires inserted through holes in the cathode and ground flush with the wave surface. These wires were glued in place and insulated from the rest of the cathode with epoxy cement. The pattern of test electrodes used in the experiments is shown in Figure 4. A final inspection with a microscope indicated that thirty-three of the forty one point electrodes were in suitable condition and that all had a diameter of 0.064 cm.

The properties of the electrolyte used in the experiments are summarized in Table 1. The diffusivity D of the I_3^- ion was calculated from the following correlation of available data (Lee, 1975):

$$\log_{10}(D) = -1.07291 \log_{10}(\nu) - 7.15278 \quad (46)$$

where D and the kinematic viscosity ν are expressed in the units of square centimeters per second.

CHARACTERIZATION OF THE VELOCITY FIELD

Measurements of the average velocity profile and the friction factor with a flat surface in place of the wave section gave results in agreement with those reported in other laboratories. These are discussed in the thesis by Thorsness (1975). The logarithmic portion of the velocity profile is represented reasonably well with

$$U = \frac{1}{0.41} \ln(y) + 5.0 \quad (47)$$

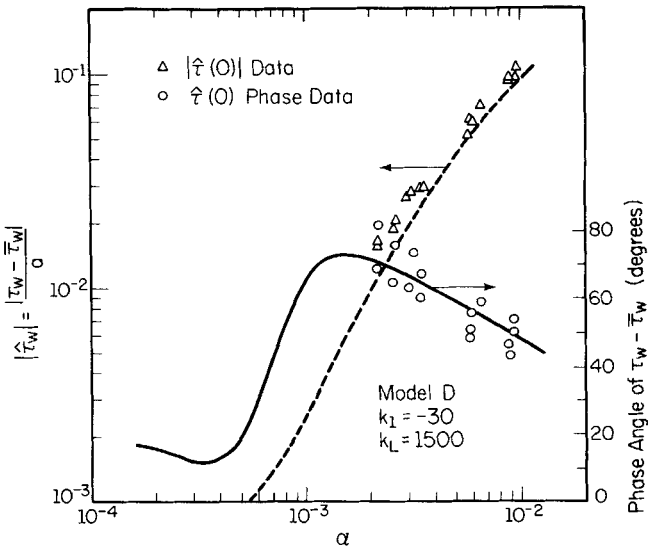

Fig. 6. Amplitudes and phase angles of the shear stress variation for turbulent flow over a surface with waves of small amplitude.

which is consistent with the use of $A = 25$ and $\kappa = 0.41$ in the Van Driest eddy viscosity relation.

Measurements of the shear stress variation along the wave surfaces were also made prior to carrying out the mass transfer experiments. These are reported in the paper by Thorsness, Morrisroe, and Hanratty (1978) and summarized in Figures 5 and 6. All of the measurements of the variation of the local wall shear stress showed a maximum upstream of the wave crest, as indicated in the sample run in Figure 5. A linear behavior was found in that the average wall shear stress over the wave surface is the same as measured for a flat surface. If a sine function is fitted to the variation of the wall stress about the average, the wave induced variation in the wall stress can be represented by an amplitude and a phase angle relative to the wave surface. Figure 6 summarizes measurements over a range of Reynolds numbers made with two different wave surfaces with amplitudes of $a = 0.0290$ cm, $a = 0.03175$ cm, and with wavelengths of 5.08 cm. The curves drawn in Figure 6 were calculated using (33), (34), (35), and (36) with $k_1 = -30$ and $k_L = 1\,500$ to calculate the eddy viscosity.

COMPARISON OF HEAT AND MASS TRANSFER EXPERIMENTS WITH CALCULATIONS

Mass Transfer Results ($Z = 729$)

The average mass transfer $\overline{N}$ to the wave surface was compared in the thesis by Thorsness (1975) with fully developed mass transfer measurements to the wall of a pipe by Shaw and Hanratty (1977) who experimented with the same electrochemical system. The agreement is good enough to support the notion that a linear response was obtained with the wave surface.

A typical profile of the measured mass transfer variation along the wave surface is shown in Figure 7. By comparing these results with those in Figure 5, it is seen that the maximum mass transfer rate is displaced slightly upstream of the wall shear stress maximum. The average mass transfer rate calculated from these profile measurements is about 10% larger than that obtained by measuring the electric current flowing to the entire mass transfer section. This is believed due to the presence of inactive epoxy around the point electrodes.

The curve shown in Figure 7 is the best fit of a sinusoidal relation to the variation of the mass transfer rate

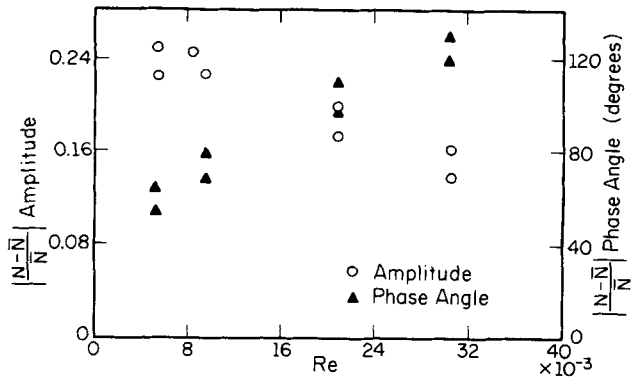

Fig. 8. Measured amplitudes and phase angles of the mass transfer variation as a function of Reynolds number.

around the average. The contribution to the measured mass transfer rates from any asymmetry in the wave surface was checked by reversing the wave section for a number of runs. No significant difference was noted in the mass transfer profiles interpreted as a single harmonic as required by the assumption of a linear response.

The amplitudes and phase angles of all of the mass transfer profiles are plotted in Figure 8. Here the average mass transfer rate $\overline{N}$ used in normalizing the data is the average of the values from the point electrodes. The same behavior as indicated for the shear stress profile in Figures 5 and 6 is found for the mass transfer profile. The relative amplitude decreases with increasing Reynolds number, and the phase angle decreases.

The relative amplitude and phase angle are plotted in Figure 9 against the wave number made dimensionless using the friction velocity and the kinematic viscosity. The effect of Reynolds number shown in Figure 9 is presented through its influence on the dimensionless wave number α.

Heat Transfer Results for $Z = 13.7$

Heat transfer data for $Z = 13.7$ were obtained from the measurements of melting ice by Ashton and Kennedy (1972). The melting occurs because of convective heat transfer from the water flowing over the ice surface and because of conductive heat transfer through the ice surface. Calculations presented by Thorsness (1975) indicate that conduction has a negligible effect. Consequently, the local variation in the surface profile is related directly to the local temperature gradient in the fluid at the ice surface.

The single datum point obtained from the data of Kennedy and Ashton is shown in Figure 9. The good agreement between the mass transfer measurements at $Z = 729$ and the heat transfer measurements at $Z = 13.7$ would suggest that the Prandtl number or Schmidt number does not have a strong effect.

A Comparison of Experimental Results with Linear Theory

Since Thorsness, Morrisroe, and Hanratty (1978) had found that the mixing length model of Loyd, Moffat, and Kays did a satisfactory job in describing wave induced variations of wall shear stress, we compare the measurements in Figure 9 with solutions of (12) using (32), (33), (34), (35), and (36) with $Z_T = 1$ to describe the wave induced variation of the Reynolds transport. The wave induced velocity field was calculated using the methods outlined by Thorsness et al. (1978) and the variation of $\overline{U}$ and $\overline{S}$, with (26), (27), and (28). The parameters used in these calculations ($\overline{A} = 25$, $\kappa = 0.41$,

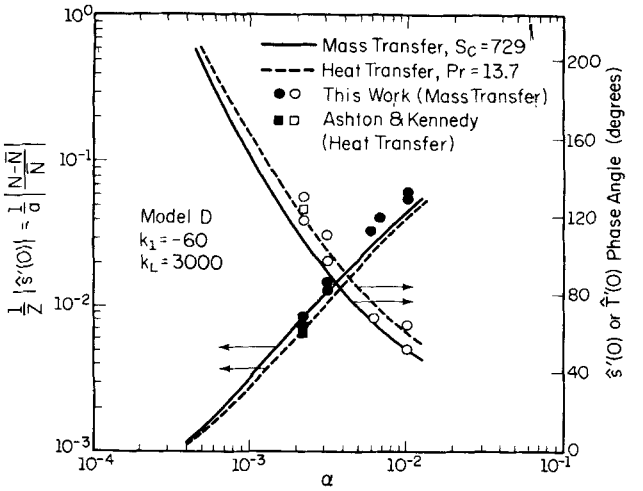

Fig. 9. Amplitudes and phase angles of the mass transfer or heat transfer variation.

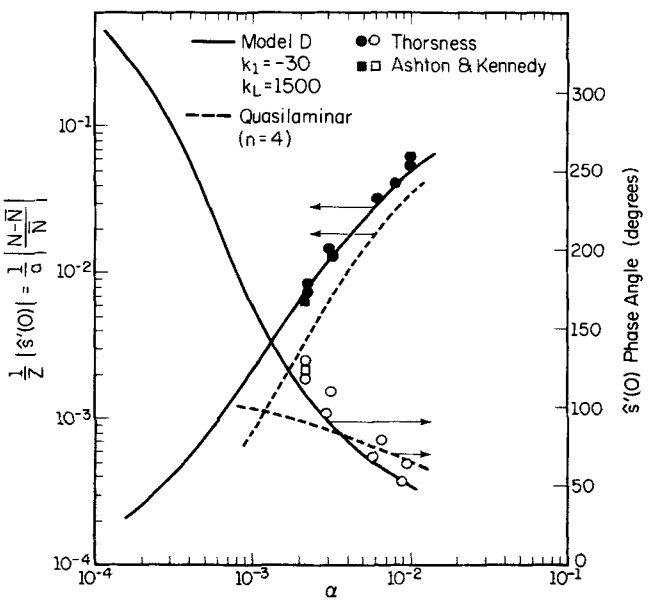

Fig. 10. Comparison of the quasilaminar model with model D for $Z = 729$.

$k_1 = -60$, and $k_L = 3\,000$) give the same fit to shear stress profile as is indicated in Figure 6.

The calculated curves in Figure 9, based on linear theory and the turbulence model of Loyd, Moffat, and Kays, do a good job in predicting the measurements.

In Figure 10, we compare calculations for $Z = 729$ using a quasilaminar model for both the wave induced velocity field and the wave induced concentration field with calculations using model D with $k_1 = -30$ and $k_L = 1\,500$. This involved solutions of the linearized mass balance Equation (12) with $\hat{m} = 0$ and the linearized momentum balance equation (Thorsness et al., 1978) with the wave induced changes in the Reynolds stress set equal to zero. The average velocity and scalar fields used in these calculations are obtained from (26), (27), and (28) with $\kappa = 0.41$ and $A = 25$. It is noted that the turbulent model is clearly superior to the quasilaminar model.

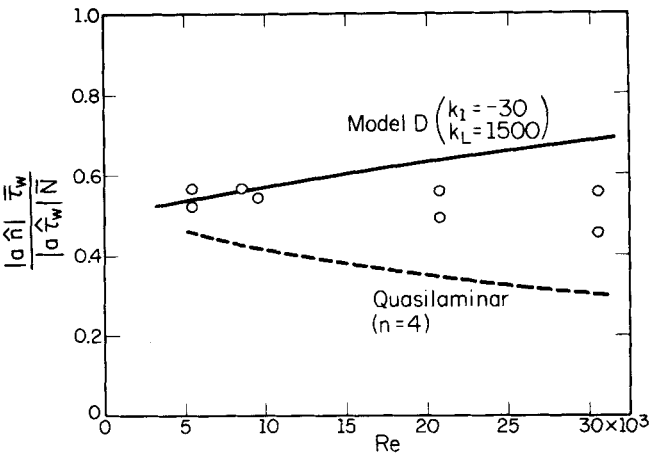

Fig. 11. Comparison of measurements of $\left|\frac{\hat{c}'(0)\bar{\tau}(0)}{\bar{C}'(0)\hat{\tau}(0)}\right|$ with calculations.

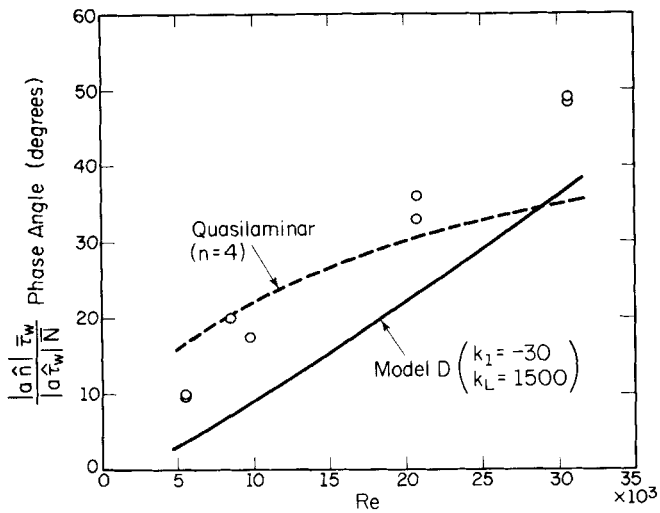

Fig. 12. Comparison of the measured phase angle of $\left|\frac{\hat{c}'(0)\bar{\tau}(0)}{\bar{C}'(0)\hat{\tau}(0)}\right|$ with calculations.

COMPARISON OF THE QUASILAMINAR AND TURBULENCE MODEL FOR MODELING THE WAVE INDUCED VARIATION OF TURBULENT MASS TRANSFER

The comparison of the measurements of wall shear stress profiles (Figure 5) with the measurements of the mass transfer profiles (Figure 7) and the calculations for laminar flows indicates that the phase and the amplitude of mass transfer rate are strongly related to the phase and the amplitude of the variation in the wall shear stress variation. Consequently, the superiority of the turbulent model over the quasilaminar model in predicting the measured mass transfer profiles can be largely ascribed to its superiority in predicting the wave induced velocity field, already demonstrated by Thorsness, Morrisroe, and Hanratty (1978). It is, therefore, of interest to compare the calculations with measured values of the relative amplitudes and phases of $\hat{n}/\bar{N}$ and $\hat{\tau}_W/\bar{\tau}_W$, since this would be more sensitive to the accuracy with which the wave induced variation in turbulent transport $\hat{m}$ is modeled. This is possible for the mass transfer measurements presented in this paper, since shear stress profiles were determined on the same waves with which the mass transfer experiments were conducted. Such a comparison is given in Figures 11 and 12.

REPRESENTATION OF THE WAVE INDUCED EDDY DIFFUSIVITY FOR LARGE SCHMIDT NUMBERS

A number of attempts were made to improve the agreement between calculations and measurements shown in Figures 11 and 12. From this work, we have tentatively concluded that the principal source of error is the use of the analogy, whereby it is assumed that

$$\frac{\hat{\epsilon}}{\bar{\epsilon}} = \frac{\hat{\nu}_T}{\bar{\nu}_T} \tag{29}$$

In order to facilitate our discussion of these efforts, we consider a simplified version of the mass balance equation valid for large Schmidt number.

The approach taken in this paper has been to represent the amplitude of the wave induced variation in the Reynolds transport coefficient $\hat{m}$ by means of a wave induced variation in the amplitude of an eddy diffusion coefficient $\hat{\epsilon}$ defined through the equation

$$\hat{m} = \frac{\bar{\epsilon}}{\nu}\hat{s}' + \frac{\hat{\epsilon}}{\nu}\bar{S}' \tag{48}$$

If this is substituted into (12), and if the concentration boundary layer is assumed to be thin enough that

$$\hat{v}(y) = \hat{v}''(0)\frac{y^2}{2} = -i\alpha\frac{\hat{\tau}_W}{\bar{\tau}_W}\frac{y^2}{2} \tag{49}$$

$$\bar{U} = y \tag{50}$$

then the linearized mass balance equation can be written as

$$i\alpha y\hat{s} - \left[\left(\frac{1}{Z} + \frac{\bar{\epsilon}}{\nu}\right)\hat{s}'\right]' = i\bar{S}'\frac{y^2}{2}\frac{\hat{\tau}_W}{\bar{\tau}_W} + \left(\frac{\hat{\epsilon}}{u^*}\frac{\nu}{\bar{\epsilon}}\frac{\bar{\epsilon}}{\nu}\bar{S}'\right)' \tag{51}$$

to be solved for $\hat{s} = 0$ at $y = 0$ and at $y = \infty$. The first term on the right side of (51) represents the influence of wave induced variations of the velocity normal to the surface on the scalar field. It is the sole cause of wave induced variations in the scalar quantity for laminar flows and for turbulent flows at large α. Equation (51) differs from the expression developed for large α previously because $\bar{S}(y)$ is not taken to be a linear function of y and because of the appearance of two turbulence terms. One of these, $\overline{\epsilon s}'$, represents a dampening of $\hat{s}$ in addition to that due to molecular diffusion. The other represents the forcing function for variations in the scalar field because of wave induced variations of the flow field. For $\alpha \to 0$, the simplifying assumption outlined previously is equivalent to assuming

$$\frac{\nu}{u^*}\frac{\hat{\epsilon}}{\bar{\epsilon}} = 2\frac{\hat{\tau}_W}{\bar{\tau}_W} \tag{52}$$

For large Z, the turbulent diffusion coefficient is usually

represented by the power law

$$\frac{\bar{\epsilon}}{\nu} = by^n \tag{37}$$

It might be reasonable to assume for large Z that $\hat{\epsilon}$ is also given by a power law with the same exponent on y. Then, for $Z \to \infty$, it would follow that $\nu\hat{\epsilon}/u^*\bar{\epsilon}$ = constant.

The influence of turbulence on the wave induced mass transfer variations enters through the specification of $\bar{\epsilon}/\nu$ and $\nu\hat{\epsilon}/u^*\bar{\epsilon}$. Thorsness (1975) has examined a number of relations for $\bar{\epsilon}$ and concluded that the calculations are insensitive to the choice of this function provided it is reasonably consistent with measurements of the average heat or mass transfer rate.

Because of this apparent insensitivity of the calculations to the choice of $\bar{\epsilon}/\nu$, considerably more effort was spent in obtaining improved relations for $\hat{\nu}_T/\nu u^*$. Thorsness (1975) used several different turbulence models to evaluate $\hat{\nu}_T/\nu u^*$. A comparison of the calculated amplitude and phase of the wave induced variation of the mass transfer rate with measurements for $Z = 729$ led him to conclude that the models for $\hat{\nu}_T/\nu u^*$ which were most accurate in predicting the wave induced variation of the wall shear stress did the best job in predicting the wave induced variation in the mass transfer rate. This is the reason for using the model of Loyd, Moffat, and Kays in this paper.

According to the eddy viscosity relation (33) used by Loyd, Moffat, and Kays, $\hat{\nu}_T$ is influenced by wave induced variations in the velocity field through the strain term e_{xy} in the pressure gradient through the dimensionless damping length A and in the wall shear stress through $\tau_W/\bar{\tau}_W$, also appearing in the damping term. Loyd, Moffat, and Kays relaxed only the influence of pressure gradient. For $\alpha k_L = 0$, their model predicts that the eddy viscosity adjusts immediately to the equilibrium value appropriate to the local pressure gradient. For large αk_L, the influence of the pressure gradient is reduced. We have explored a modified version of Loyd, Moffat, and Kays model for which the influence of the local wall shear stress, as well as the pressure gradient, on the mixing length is relaxed. For large Z, it is only necessary to consider the first term of a power series expansion of a linearized form of this eddy viscosity function:

$$\frac{\hat{\nu}\hat{\epsilon}}{u^*\bar{\epsilon}} = \frac{\hat{\nu}_T\nu}{\bar{\nu}_T u^*}$$

$$= \frac{\tau_W}{\bar{\tau}_W}\left[1 + \frac{1}{1 + i\alpha k_{L\tau}} - \frac{2i\alpha k_1}{1 + i\alpha k_{LP}}\,\frac{\hat{p}(0)\,\bar{\tau}_W}{\hat{\tau}_W}\right] \tag{53}$$

The first term on the right represents the influence of wave induced variations of the rate of strain, and the second and third terms represent the influence of wave induced variations of the wall shear stress and pressure on the damping of the mixing length close to the wall. The terms k_{LP} and $k_{L\tau}$ are the relaxation constants for the influences of pressure gradient and wall shear stress on the mixing length.

The calculations shown in Figures 11 and 12 are based on (53), using values of $k_{L\tau} = 0$, $k_1 = -30$, and $k_{LP} = 1\,500$. A number of attempts to improve the agreement with the measurements were made by using different values of $k_{L\tau}$, k_1, and k_{LP}. Significant improvements could be obtained only by using nonzero values of $k_{L\tau}$. This would suggest that the Loyd, Moffat, and Kays model predicts too strong an influence of $\hat{\tau}_W$ on the wave induced mass transfer rates at large α.

However, in every case, models for $\hat{\nu}_T/\bar{\nu}_T$ which yielded improved agreement with mass transfer measurements also yielded poorer agreement with the measurements of the wave induced variation in the wall shear stress than is indicated in Figure 6. One possible explanation for these calculated results is that the analogy as stated in (29) is inadequate.

CLOSURE

An analysis of the wave induced variation of the mass transfer rate along a solid surface has been presented for the case of a laminar boundary layer on a flat plate at large Schmidt numbers. As can be seen from the results of a sample calculation shown in Figure 2 and from (16), the predicted ratio of the amplitude of the mass transfer variation to the average mass transfer rate can be as large as 0.2 a at large α. The decrease in the amplitude of the mass transfer variation with decreasing wave number can be explained by the decrease in the magnitude of the wave induced variations of the velocity normal to the surface. The maximum in the mass transfer rate was calculated to be from 30 to 70 deg upstream of the wave crest. Larger values of the phase shift could be calculated, but these would be unrealistic conditions where the wavelength of the wave is larger than the length of the plate. The strong influence of the shear stress variation along the wave surface is illustrated by the result that the mass transfer ratio $a|\hat{n}|\,\bar{\tau}_W/a|\hat{\tau}_W|\,\bar{N}$ is approximately equal to 0.5.

Turbulent flows differ from laminar flows in that the wall shear stress variation is quite different and in that the wave induced variation of the Reynolds transport is another mechanism to cause changes in the mass transfer rate along the surface. Special solutions for large α and for small α indicate that the accurate evaluation of the Reynolds transport terms is particularly important at intermediate α. In previous work, it has been found that a model developed by Loyd, Moffat, and Kays for the eddy viscosity does a reasonable job in predicting the shear stress variation. This model incorporates the experimental observation that turbulence close to a boundary is damped in regions having favorable pressure gradients. Thus, it predicts that the wave induced pressure variations at the wave surface play a principal role in governing turbulent transport at wavy surfaces. We use this model and the assumption that the eddy diffusivity for heat and mass is directly proportional to the eddy viscosity in order to calculate turbulent mass transfer and heat transfer to wavy surfaces. Good agreement is obtained with our own mass transfer experiments at Schmidt number of 729 and with the heat transfer experiments by Ashton and Kennedy at a Prandtl number of 13.7.

Of particular interest in the application which motivated this research is the finding that for turbulent flows the phase of the mass transfer variation can be larger than 90 deg. Consequently, there is a range of α for which the maximum in the mass can exist in the trough of the wave. This suggests that for turbulent flows, planar dissolving surfaces can be unstable. A discussion of this stability problem is presented in another paper.

A closer examination of the mass transfer results obtained at a Schmidt number of 729 reveals that the calculations were successful because they are based on a model which does a good job in predicting the wall shear stress variation. A detailed analysis of the sensitivity of the calculations to parameters of the model has been carried out by Thorsness (1975). The approximate analysis for large Schmidt numbers developed in the previous section clearly shows through (51) and (53) that the evaluation of the mass transfer variation is strongly related to the wall shear stress variation. It is found that the calculations based on this approximate equation are not sensitive to the specified spatial variation of the average concentration over a flat plate. Modifications of the parameters appearing in the Loyd, Moffat, and Kays eddy viscosity that were found to improve the ratio of the mass transfer variation to the wall shear stress variation gave poorer agreement with the wall shear stress measurements. It appears to us that a more fruitful approach for improving the evaluation of the wave induced variation of the turbulent transport of heat or mass would require the abandonment of the analogy whereby the eddy diffusivity is related to the eddy viscosity.

ACKNOWLEDGMENT

This work is being supported by the National Science Foundation under grant NSF ENG 76-22969.

NOTATION

a = wave amplitude normalized using u^* and ν
$a|\hat{n}|$ = amplitude
A = Van Driest parameter defined by Equation (35)
A_0 = Van Driest parameter for zero pressure gradient
A_e = area of the electrode (m^2)
Ai = Airy function
$Ai(z)$ = Airy function of complex variable z
b = constant defined by Equation (37)
C_P = heat capacity, J/kg °K
D = diffusion coefficient, m^2/s
e_{xy} = component of rate of strain tensor normalized using u^* and ν
F = Faraday's constant
h = heat transfer coefficient
h_x, h_y = metrics for the curvilinear coordinate system x, y
I = electric current flowing to the electrode
K = mass transfer coefficient, m/s
k_1 = constant characterizing the influence of the pressure gradient on the Van Driest parameter A, as defined by (35)
k_L = relaxation constant defined by (36)
$k_{LP}, k_{L\tau}$ = relaxation constants defined by (53)
L = mixing length normalized using u^* and ν
M = Reynolds transport term normalized using u^* and $\overline{N}$
$\hat{m}a$ = amplitude of the wave induced variation of M
N = mass or heat flux to surface made dimensionless using the average flux; that is, $\overline{N} = 1$. In (2) it is dimensional
$\overline{N}$ = spatially averaged mass flux
n_e = number of electrons involved in the reaction
$\hat{n}a$ = amplitude of the wave induced variation of N
P = dimensionless pressure
Re_x = Reynolds number
S = concentration relative to that at the wall normalized using u^* and $\overline{N}$
S_w = value of S at the wall
S_∞ = value of S far from the surface
$\hat{s}a$ = amplitude of wave induced variation in S
U = velocity component in the x direction normalized using u^*
U_∞ = velocity at large distances from the surface
$\hat{u}a$ = amplitude of wave induced variation in U
u^* = friction velocity equal to $(\overline{\tau}_W/\rho)^{1/2}$
V = velocity component in the y direction normalized using u^*
$\hat{v}a$ = amplitude of wave induced variation in V
X, Y = Cartesian coordinates
x, y = boundary-layer coordinates normalized using u^* and ν
y^* = $(\alpha Z)^{1/3}y$
Z = Schmidt number or Prandtl number
Z_T = turbulent Schmidt number or Prandtl number

Greek Letters

α = wave number normalized using u^* and ν except in (1) and (2) where it is not normalized
δ = thickness of the velocity boundary layer normalized using u^* and ν
δ_c = thickness of the concentration boundary layer normalized with u^* and ν
δ_c^* = $(\alpha Z)^{1/2}\delta_c$
ϵ = turbulent diffusivity for heat or mass, m^2/s
$\hat{\epsilon}$ = amplitude function defined by (30), m/s
θ = phase angle to be defined by (1) and (2)
κ = von Karman constant
λ = wavelength normalized using u^* and ν
ν = kinematic viscosity
ν_T = turbulent viscosity, m^2/s
$\hat{\nu}_T$ = amplitude function defined by (31), m/s
ρ = density, kg/m^3
τ_W = shear stress acting on the wave surface normalized with the average wall stress, that is, $\tau_W = 1$
$\hat{\tau}_W a$ = amplitude of wave induced variation in τ_W
Ω = $\alpha^{n/3}Z^{(n-3)/3}/b$

Other Symbols

$|N|$ = $(R^2 + I^2)^{1/2}$, where R and I are the real and imaginary parts of N
$\overline{N}(y)$ = average value of N over one wavelength
$N'(y)$ = derivative of N with respect to y

LITERATURE CITED

Allen, R. W., and E. R. G. Eckert, "Friction and Heat Transfer Measurements to Turbulent Pipe Flow of Water ($Pr = 7$ and 8) at Uniform Wall Heat Flux," *Trans. Am. Soc. Mech. Engrs.*, 86, 301 (1964).

Ashton, G. D., and J. F. Kennedy, "Ripples on Underside of River Ice Covers," *J. Hydraulics Division, Proc. A.S.C.E.*, 98, 1603 (1972).

Benjamin, T. B., "Shearing Flow Over a Wavy Boundary," *J. Fluid Mech.*, 6, 161 (1959).

Harriot, P., and R. M. Hamilton, "Solid-Liquid Mass Transfer in Turbulent Pipe Flow," *Chem. Eng. Sci.*, 20, 1073 (1965).

Hubbard, D. W., "Correlation of Mass Transfer Data: Comments on an Article by Son and Hanratty," *AIChE J.*, 14, 354 (1968).

Hughmark, G. A., "Notes on Transfer in Turbulent Pipe Flow," *ibid.*, 18, 1072 (1972).

Lee, M., "Turbulent Wall Eddy Structure and the Reynolds Stress in the Wall Region of a Pipe Flow," Ph.D. thesis, Univ. Ill., Urbana (1975).

Loyd, R. J., R. J. Moffat, and N. M. Kays, *Rept. No. HMT-13*,

Thermosciences Division, Department of Mechanical Engineering, Stanford Univ., Calif. (1970).
Shaw, D. A., and T. J. Hanratty, "Turbulent Mass Transfer Rates to a Wall for Large Schmidt Numbers," *AIChE J.*, 23, 28 (1977).
Thorsness, C. B., "Transport Phenomena Associated with Flow over a Solid Wavy Surface," Ph.D. thesis, Univ. Ill., Urbana (1975).
———, P. E. Morrisroe, and T. J. Hanratty, "A Comparison of Linear Theory with Measurements of the Variation of Shear Stress Along a Solid Wave," *Chem. Eng. Sci.*, 33, 579 (1978).
Thorsness, C. B., and T. J. Hanratty, "Turbulent Flow Over Wavy Surfaces," in *Symposium on Turbulent Shear Flows*, Vol. 1, University Park, Pa. (1977).
Verma, S. B., and J. E. Cermak, "Mass Transfer From Aerodynamically Rough Surfaces," *Intern. J. Heat Mass Transfer*, 17, 567 (1974).

Manuscript received January 13, 1978; revision received March 12 and accepted March 23, 1979.

Stability of Dissolving or Depositing Surfaces

C. B. THORSNESS
and
THOMAS J. HANRATTY
Department of Chemical Engineering
University of Illinois
Urbana, Illinois

In a previous paper, we have examined the variation of the mass transfer rate along a small amplitude wavy surface which is exchanging mass with a turbulently flowing fluid. We now use these results to show that a soluble flat surface is unstable in the presence of a turbulent flow. The wavelength of the most rapidly growing surface disturbance, made dimensionless with respect to the friction velocity and the kinematic viscosity, is found to be a very weak function of the Schmidt number. These results provide a possible explanation for wavelike dissolution patterns observed in caves and on the underside of river ice. The analysis predicts that deposition patterns should be quite different from dissolution patterns in that the most rapidly growing wave for deposition has a length of zero.

SCOPE

In this paper, we use results obtained in our laboratory on mass transfer to wavy surfaces to examine the stability of an initially flat surface which is dissolving or growing in a turbulent flow. A wavelike disturbance pattern with crests normal to the direction of mean flow is examined. Ranges of wavelengths are predicted over which disturbances on dissolving or depositing surfaces will grow. In addition, it is argued that the wavelength that eventually develops is close to that of the fastest growing wave.

The final wave pattern that develops on a dissolving surface is governed by nonlinear effects, such as flow separation, so that the linearized equations of stability theory are no longer applicable. By comparing predictions from stability theory with dissolution patterns observed in caves, we examine whether the final observed spacing between crests is determined by the stability of the surface, rather than the nonlinear effects. Therefore, stability theory can be used to predict the influence of system variables on the wavelength and velocity of dissolution patterns that initially appear on a dissolving surface and, perhaps, the wavelength of the final pattern.

CONCLUSIONS AND SIGNIFICANCE

The stability analysis of a surface dissolving in the presence of a turbulent flow shows that wavelike patterns can appear for wavelengths greater than a certain critical value. The wavelength of the most rapidly growing surface disturbance, made dimensionless with respect to the friction velocity and the kinematic viscosity, is found to be a very weak function of the Schmidt number. The wavelength of maximum growth is close to the wavelength of dissolution patterns observed in limestone caves and on melting ice. This comparison suggests that these patterns can be explained by a stability mechanism. For deposition processes, waves can occur, provided the wavelength is below the critical wavelength for the dissolution process. However, in this case the wavelength of maximum growth is zero. This suggests that deposition would be accompanied by a pattern with very small wavelength, possibly so small that it cannot be seen.

0001-1541-79-2712-0697-$00.75.